Journal of Solid Mechanics Vol. 16, No. 2 (2024) pp. 168-180
DOI: 10.60664/jsm.2024.3121798

Research Paper

Post-Buckling Analysis of Porous Circular Plate with Small Initial Deflection Using First-Order Shear Deformation Theory

M. Alimohammadi, M.M. Ghomshei *

Department of Mechanical Engineering, Karaj Branch, Islamic Azad University, Karaj, Iran

Received 22 December 2023; Received in revised form 4 September 2024; Accepted 14 September 2024

ABSTRACT

In this study, buckling and post-buckling analysis of circular porous plate with small initial deflection is investigated using the first-order shear deformation theory. Porosity is assumed variable in the thickness of the plate, and assumed to be symmetric with respect to the plate mid-plane. The first-order shear deformation theory and nonlinear von-Karman strain field has been used to derive the equilibrium equations in term of displacement field. The governing differential equations together with the boundary conditions are discretized by implementing the differential quadrature method (DQM). The set of nonlinear algebraic equations are then solved for displacement field components using an iterative method. The convergence of the numerical model is surveyed. Then the comparative and parametric studies are carried out. The results show that the present DQM model has fast convergence, and accurate results. Moreover the porosity factor and initial deflection have significant influence on the plate deformation.

Keywords: Porous circular plate; Small initial deflection; Differential quadrature method (DQM); Buckling and post-buckling; First-order shear deformation theory.

1 INTRODUCTION

RECENT advances in material science make progresses in different high technology industries such as aerospace, military, nuclear, medicine, etc. Achievement to the knowledge of the advanced materials is become more and more important for the industries. For this reason, academic researches are conducted to produce and develop these materials, with their applications in structural design. Porous materials are advanced materials that have voids or pores in their structure, which may be empty or filled with a fluid. Porous materials have excellent

*Corresponding author. Tel.: +98 26 34259571-9.
E-mail address: mm.ghomshei@iau.ac.ir (M.M.Ghomshei)

properties including lightness, flexibility, and resistance to hairline cracks, which impel the industries to make use of them in structural design [1].

Ma and Wang [2] investigated the nonlinear bending and post-buckling of a circular functionally graded plate under mechanical and thermal loads. They studied the effects of material constants and boundary conditions on the temperature distribution, nonlinear bending, critical buckling temperature and post-buckling thermal behavior of FGM plate. Magnucki and Stasiewicz [3] investigated the elastic buckling of a porous beam using classical theory and examined the effect of porosity on the beam buckling load.

Samsam Shariat and Eslami [4] investigated the thermal buckling of rectangular functionally graded plates with initial geometrical imperfections using first order shear deformation theory. The plate is assumed to be under three types of thermal loading, namely: uniform temperature rise, nonlinear temperature rise through the thickness, and axial temperature rise. Resulting equations are employed to obtain the closed-form solutions for the critical buckling temperature change of an imperfect functionally graded plate. Jalali and Naei [5] investigated the buckling response of homogeneous circular plates with variable thickness subjected to radial compression based on the first-order shear deformation plate theory in conjunction with von-Karman nonlinear strain-displacement relations. They examined the influence of the boundary conditions, the thickness variation profile and aspect ratio on the buckling behavior. Alipour and Shariyat [6] studied the bending behavior and stress distribution of two-directional functionally graded FG circular plates resting on non-uniform two-parameter foundations using the first-order shear-deformation theory. They concluded that in contrast with the available constitutive-law-based solutions, their solution guarantees continuity of the transverse stresses at the interfaces between layers and may also be used for stress analysis of the sandwich panels. Magnucki et al. [7] on a study on the bending and buckling of a rectangular porous plate using classical theory, concluded that the non-linear symmetric distribution of porosity in the plate have better resistance. Jabari et al. [8] investigated porous circular functionally graded plates using higher order shear deformation theory and obtained the critical buckling loads. Kamranfard et al. [9] in their study of the buckling of porous annular sector plates investigated the influence of different geometrical parameters such as section angle, thickness, plate internal radius and also the amount of porosity of the plate on the critical load of buckling. Tu et al. [10] in their nonlinear buckling and post-buckling studies of porous plates with defects under mechanical loads extracted results which indicate that the critical buckling load in the porous plate decreases with increasing porosity, FGM plates with symmetrical porosity distribution have better resistance against mechanical loads and also the plates with defects have more post-buckling deflections than perfect plates. Bagheri et al. [11] studied the asymmetric thermal buckling of temperature dependent annular FGM plates on a partial elastic foundation and presented their results proportional to the stiffness of the elastic foundation. In another article, Jabbari et al. [12] in their investigation on the axially symmetric buckling of the saturated porous circular plate using the first-order shear deformation theory, have come to the conclusion that increase in the size of the pores, porosity and thickness of the plate leads to a decrease in stability. Moreover the plate with symmetric distribution of the pores shows a more stable behavior, besides the reduction of the fluid compressibility inside the pores increases the stability of the plate. A numerical solution formulation based on the DQM is developed by Ghomshei [13] for axisymmetric thermal buckling analysis of variable thickness FGM moderately thick circular plates resting on Pasternak foundation, based on FSDPT and von-Karman strain field. The fast convergence, validation and high accuracy of the proposed DQ formulation are investigated. Parametric surveys are carried out with focus on the effect of thickness variations and bed parameters on the plate thermal buckling factor and the 1st mode shape of buckling. Khorshidvand and Kolahi [14] investigated the effects of porosity and radius ratio on the deflection of a buckled circular porous plate and concluded that the deflection increases with the increase of the porosity factor, while the deflection decreases with the increase of the radius ratio. Njim et al. [15] in an analytical and numerical investigation on the buckling load of functionally graded materials with porous metal sandwich plate, studied the effects of porosity index, elastic parameters, porosity ratio and length-to-thickness ratio on the buckling stresses by using classical theory. Zenkour and Aljadani [16] studied porous plates made of functionally graded materials, using the method of modified Quasi-3D refined theory. They fully explained the effect of porosity on the critical load of buckling and post-buckling created in the plate. Sheplak and Dugundji [17] studied the large deflections of clamped circular plates under initial stress and the transition to membrane behavior. They presented the results, values and trends in a general, dimensionless way and showed that the results are useful for the design of circular thin disks in micro sensor applications.

In the current research, the axisymmetric post-buckling of porous circular plates with small initial deflection and variable porosity distribution through thickness is studied. The porosity distribution is so that the highest porosity is in the middle plane and the lowest porosity is in the upper and lower surfaces. The plate with a small initial deflection is subjected to a uniform in-plane radial load. The governing equations in terms of displacement field are derived based on the first-order shear deformation theory with von-Karman strain field. To solve the equations the differential quadrature method is used to discretize the equations. The obtained set of nonlinear algebraic equations

is then solved for displacement field components using an iterative method. The convergence of the numerical model is examined. Then the comparative and parametric studies are carried out. The results show that the present DQM model has fast convergence, and accurate results.

2 BASIC EQUATIONS AND FORMULATION

2.1 Plate parameters

A porous plate with radius R and thickness h is considered, where the coordinate axis r is located in the mid-plane of the plate and the coordinate axis z is located along the thickness of the plate. The plate defected by a small initial deflection w_0 . The porosity is assumed to be variable along the z axis, so the elastic modulus varies according to the porosity along the thickness of the plate. Geometric parameters of the porous circular plate are as shown in Fig. 1.

The plate porosity distribution assumed to have symmetry with respect to mid-plane and has a non-linear with cosine distribution in thickness. So that the elastic and shear moduli of the plate material have symmetry with respect to mid-plane as defined by the following equations [12]:

$$E(z) = E_s\left[1 - e_1 \cos\left(\frac{\pi z}{h}\right)\right],$$

$$G(z) = G_s\left[1 - e_1 \cos\left(\frac{\pi z}{h}\right)\right] \tag{1}$$

G_s and E_s are respectively the shear modulus and elastic modulus of the material without porosity, respectively, e_1 is the porosity parameter related to the porosity factor β as [18]:

$$e_1 = 1 - (1-\beta)^2 \quad , \quad 0 \le \beta < 1 \tag{2}$$

For the initial small deflection cosine functions is considered so that the maximum deflection exists in the middle of the plate and the deflection is zero at the outer edge of the plate. The functions for the simple and clamped boundary conditions respectively are as follows:

$$w_0 = w_c \cos\left(\frac{\pi r}{2R}\right), \qquad w_0 = w_c \cos^2\left(\frac{\pi r}{2R}\right) \tag{3}$$

2.2 Plate kinematic relations

According to the thick plate assumption, the first-order shear deformation theory is used here to estimate the displacement field in a circular plate. Based on the theory, the displacement components in cylindrical coordinates are stated as:

$$u(r,z) = u_0(r) + z\varphi(r), \qquad w(r,z) = w(r) \tag{4}$$

where u and w are the radial and lateral displacements, respectively, and φ is the total rotation around the peripheral axis, and u_0 represents the mid-plane radial displacement. Also, the strain components are written as [19]:

$$\varepsilon_r = \varepsilon_r^0 + \kappa_r z\,, \qquad \varepsilon_\theta = \varepsilon_\theta^0 + \kappa_\theta z\,, \qquad \gamma_{rz} = \varphi + w_{,r} \tag{5}$$

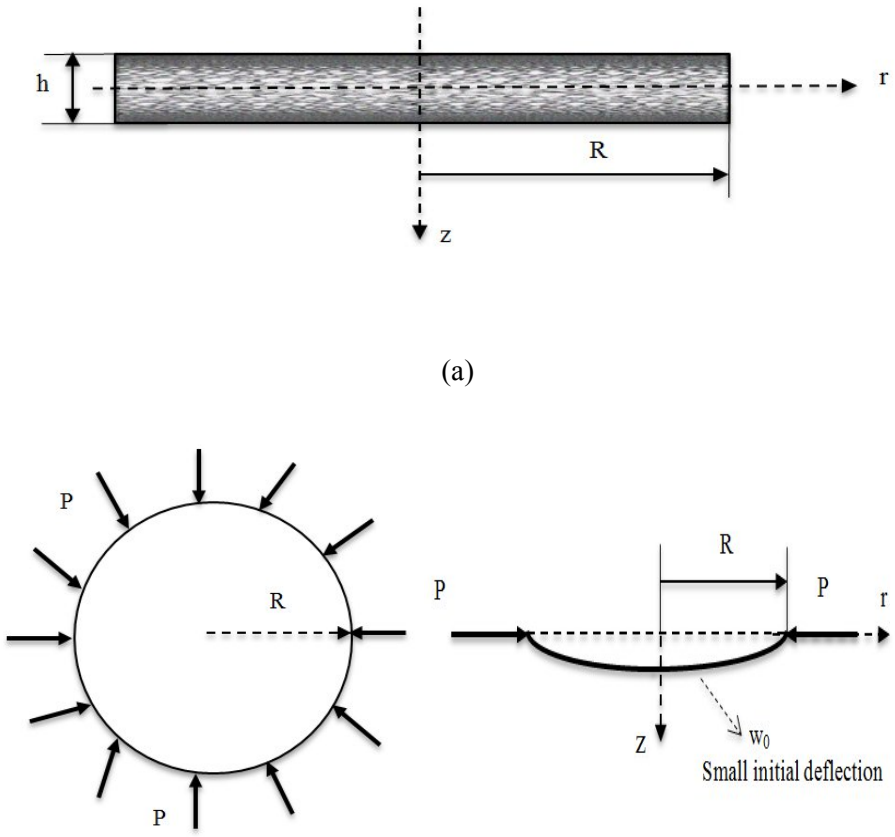

Fig. 1
Geometric parameters of the assumed porous circular plate,(a) Cross-section of plate with porosity, (b) In-plane loading on circular plate, (c) Small initial deflection of plate.

Based on von-Karman assumptions, which is suitable for relatively large deflections, the mid-plane strains ε_r^0, ε_θ^0 and the curvatures κ_r, κ_θ in terms of displacements are given as follows [19]:

$$\varepsilon_r^0 = u_{0,r} + \frac{1}{2}(w_{,r})^2, \quad \varepsilon_\theta^0 = \frac{u_0}{r}, \quad \kappa_r = \varphi_{,r}, \quad \kappa_\theta = \frac{\varphi}{r} \tag{6}$$

In Eqs (6), and from now on the derivative with respect to *r* is written as $()_{,r}$.

The stress-strain relations for porous plates assumed to follow Hook's law [20]:

$$\sigma_r = \frac{E}{1-\nu^2}(\varepsilon_r + \nu\varepsilon_\theta), \quad \sigma_\theta = \frac{E}{1-\nu^2}(\varepsilon_\theta + \nu\varepsilon_r), \quad \tau_{rz} = \frac{E}{2(1+\nu)}\gamma_{rz} \tag{7}$$

where σ_r and σ_θ are the normal stresses in the *r* and θ directions, respectively, and τ_{rz} is the shear stress, and ν is Poisson's ratio which assumed to be constant through the plate thickness.

The force/moment resultants can be calculated by the following integrations over the thickness of the plate:

$$(N_r, N_\theta) = \int_{-\frac{h}{2}}^{\frac{h}{2}} (\sigma_r, \sigma_\theta) dz, \qquad (M_r, M_\theta) = \int_{-\frac{h}{2}}^{\frac{h}{2}} (\sigma_r, \sigma_\theta) z dz, \qquad Q_r = \int_{-\frac{h}{2}}^{\frac{h}{2}} \tau_{rz} dz \tag{8}$$

By substituting Eq.(7) into Eq.(8) and integrating, we have:

$$N_r = \frac{E_1 h}{1-\nu^2}(\varepsilon_r^0 + \nu\varepsilon_\theta^0), \qquad N_\theta = \frac{E_1 h}{1-\nu^2}(\varepsilon_\theta^0 + \nu\varepsilon_r^0), \qquad M_r = \frac{E_2 h^3}{1-\nu^2}(\kappa_r + \nu\kappa_\theta),$$

$$M_\theta = \frac{E_2 h^3}{1-\nu^2}(\kappa_\theta + \nu\kappa_r), \qquad Q_r = \frac{E_1 h}{2(1+\nu)}\gamma_{rz} \div \frac{E_1 h}{1-\nu^2} = \frac{K(1-\nu)}{2}\gamma_{rz} \tag{9}$$

where K is the shear correction factor and its value is equal to $\frac{\pi^2}{12}$

We can rewrite Eq.(9) in matrix form as below:

$$\begin{Bmatrix} N_r \\ N_\theta \\ M_r \\ M_\theta \\ Q_r \end{Bmatrix} = \begin{bmatrix} A_{11} & A_{12} & 0 & 0 & 0 \\ A_{12} & A_{22} & 0 & 0 & 0 \\ 0 & 0 & D_{11} & D_{12} & 0 \\ 0 & 0 & D_{12} & D_{22} & 0 \\ 0 & 0 & 0 & 0 & A_{55} \end{bmatrix} \begin{Bmatrix} \varepsilon_r^0 \\ \varepsilon_\theta^0 \\ \kappa_r \\ \kappa_\theta \\ \gamma_{rz}^0 \end{Bmatrix} \tag{10}$$

where:

$$A_{11} = \frac{E_1 h}{1-\nu^2}, \qquad A_{12} = \frac{\nu E_1 h}{1-\nu^2}, \qquad A_{22} = \frac{E_1 h}{1-\nu^2}, \qquad A_{55} = \frac{K(1-\nu)}{2} A_{11}$$

$$D_{11} = \frac{E_2 h^3}{12(1-\nu^2)}, \qquad D_{12} = \frac{\nu E_2 h^3}{12(1-\nu^2)}, \qquad D_{22} = \frac{E_2 h^3}{12(1-\nu^2)} \tag{11}$$

$$A_{11} = A_{22}, \qquad A_{11} = \nu A_{12}, \qquad D_{11} = D_{22}, \qquad D_{11} = D_{12}$$

in that A_{ij} and D_{ij} are tensile and bending stiffness's respectively, and E_1 and E_2 are obtained by the following integrals [13]:]

$$(E_1, E_2) = 2\int_0^{\frac{h}{2}} (1, z^2) E(z) dz \tag{12}$$

2.3 Equilibrium equations

The plate equilibrium equations are obtained using the energy method as mentioned in reference [21] for the shear deformable plate. These equations are written in terms of the resultant forces and moments as below:

$$\delta u : (rN_r)_{,r} - N_\theta = -N_r w_{0,rr} - P,$$

$$\delta\varphi : rM_{r,r} + M_r - M_\theta - rQ_r = 0, \tag{13}$$

$$\delta w : \frac{1}{r}(rQ_r)_{,r} + \frac{1}{r}(rN_r w_{,r})_{,r} = 0$$

where $-N_r w_{0,rr}$ in the first of Eq. (13) is the effect of the initial small deflection which appears as an in-plane distributed radial load [22], and -*P* is an external circumferential load applied on the outer edge of the plate.

Substituting Eq.(10) into Eq.(13), then substituting from Eq.(6) into the resulting statements, the equilibrium equations are obtained in terms of displacements as follows:

$$\begin{aligned}\delta u : {} & 2r^2 A_{11} u_{0,rr} + \left(2rA_{11}\left(1 + w_{0,rr}\right)\right) u_{0,r} + \left(2A_{11}\left(\nu w_{0,rr} - 1\right)\right) u_0 \\ & + rA_{11}\left((1-\nu)w_{,r} + 2rw_{,rr} + w_{,r} w_{0,rr}\right) w_{,r} = -P\,,\end{aligned}$$

$$\delta\varphi : r^2 D_{11}\varphi_{,rr} + rD_{11}\varphi_{,r} - (D_{11} + r^2 A_{55})\varphi - r^2 A_{55} w_{,r} = 0\,. \tag{14}$$

$$\begin{aligned}\delta w : {} & 2rA_{55} w_{,rr} + \left[2A_{55} + \left(A_{11} w_{,r}\right)\left(3rw_{,rr} + w_{,r}\right)\right] w_{,r} + 2rA_{55}\varphi_{,r} + 2A_{55}\varphi + 2rA_{11} w_{,r} u_{0,rr} \\ & + 2A_{11}\left(rw_{,rr} + (1+\nu)w_{,r}\right) u_{0,r} + 2\nu A_{11} w_{,r} u_0 = 0\end{aligned}$$

3 DISCRETIZATION OF THE EQUATIONS

A numerical method known as differential quadrature method (DQM) is used to simultaneously solve the governing ODE's (Ordinary Differential Equations) of variable coefficients, in that the weighting coefficients are determined by the procedure introduced by Shu and Richards as cited in Ref. [23]. To ensure the convergence of DQ approximation, an unequally spaced grid point distribution so-called Chebyshev nodes is utilized. Applying the differential quadrature rule as mentioned in Ref. [23] to the equilibrium equations Eq. (14), the discretized forms of the equations are derived as

$$\begin{aligned}\delta u : {} & 2\eta_i^2 A_{11} \sum_{j=1}^{N} C_{ij}^{(2)} U_j^0 + \left(2\eta_i A_{11}\left(1 + w_{0,rr}\right)\right) \sum_{j=1}^{N} C_{ij}^{(1)} U_j^0 + \left(2A_{11}\left(\nu w_{0,rr} - 1\right)\right) U_j^0 \\ & + \eta_i A_{11}\left((1-\nu)w_{,r} + 2\eta_i w_{,rr} + w_{,r} w_{0,rr}\right) \sum_{j=1}^{N} C_{ij}^{(1)} W_j = -P\,,\end{aligned}$$

$$\delta\varphi : \eta_i^2 D_{11} \sum_{j=1}^{N} C_{ij}^{(2)} \Phi_j + \eta_i D_{11} \sum_{j=1}^{N} C_{ij}^{(1)} \Phi_j - (D_{11} + \eta_i^2 A_{55})\Phi_j - \eta_i^2 A_{55} \sum_{j=1}^{N} C_{ij}^{(1)} W_j = 0\,. \tag{15}$$

$$\delta w : 2\eta_i A_{55} \sum_{j=1}^{N} C_{ir}^{(2)} W_j + \left[2A_{55} + (A_{11} w_{,r})(3\eta_i w_{,rr} + w_{,r})\right] \sum_{j=1}^{N} C_{ir}^{(1)} W_j + 2\eta_i A_{55} \sum_{j=1}^{N} C_{ir}^{(1)} \Phi_j + 2A_{55} \Phi_j + 2\eta_i A_{11} w_{,rr} \sum_{j=1}^{N} C_{ir}^{(2)} U_j^0 + 2A_{11}(\eta_i w_{,rr} + (1+\nu) w_{,r}) \sum_{j=1}^{N} C_{ir}^{(1)} U_j^0 + 2\nu A_{11} w_{,rr} U_j^0 = 0$$

where $C_{ir}^{(2)}$, $C_{ir}^{(1)}$ are weighting coefficients of the second and first order derivatives respectively and N is the selected number of grid points.

Also, the discretized forms of the boundary conditions are as follows:

$$W_N = 0, \quad \sum_{j=1}^{N} C_{1j}^{(1)} \Phi_j + \nu \Phi_N = 0 \quad \text{(simple support edge)},$$

$$W_N = 0, \quad \Phi_N = 0 \quad \text{(clamped edge)}, \tag{16}$$

$$U_1 = 0, \quad \Phi_1 = 0, \quad \sum_{j=1}^{N} C_{1j}^{(1)} W_j = 0 \quad \text{(center point)}$$

4 NUMERICAL RESULTS AND DISCUSSION

Based on the DQ formulation, a computer program written in MATLAB is prepared, and the numerical results are extracted. The numerical results are concerned with the values of the plate properties: elastic modulus of solid material 210 GPa, plate thickness 0.002 meter, porosity 10%, Poisson' ratio 0.285, plate initial deflection at center point 0.005 meter and plate radius 0.5 meter, unless otherwise specified.

4.1 Convergence of the results

To study the convergence of the present numerical method, the computer program is implemented with a number of grid points including 5, 7, 9, 11, ... up to 31 points. Fig .2 shows the convergence diagram. Since the numerical method has enough accuracy with 15 grid points, the effects of various parameters of the plate have been investigated by using 15 grid points. The normalized error percent for simply support boundary condition is 0.066% and those of clamped boundary condition is 0.0756%.

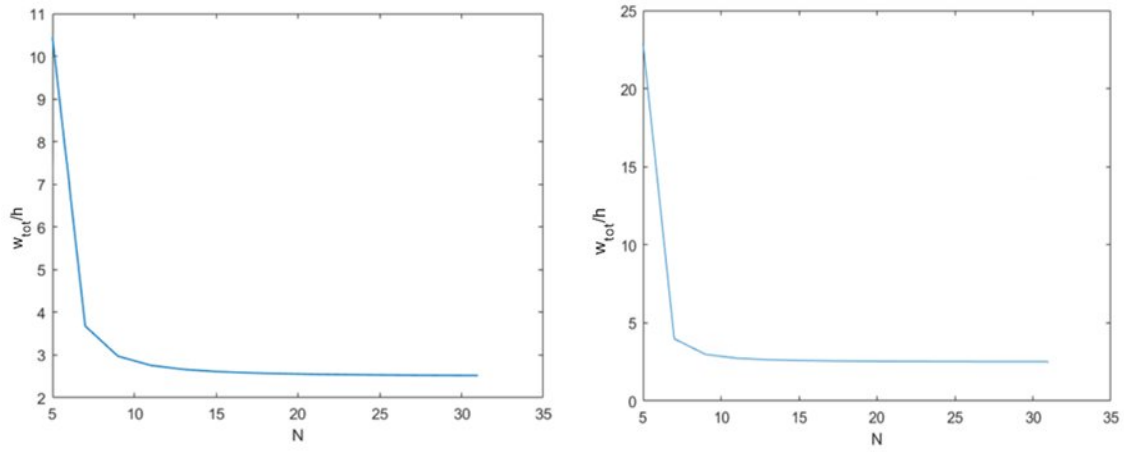

(a) (b)

Fig. 2
Dimensionless deflection vs. number of grid points for (a) clamped edge, (b) simply supported edge.

4.2 Validation

To check the accuracy of the present numerical method, we compare its numerical results with those of Ref. [2]. It should be noted that in Ref. [2] the results are obtained for the case without porosity and initial deflection. So, here by considering the zero porosity and zero initial deflection with the material and elastic modulus used same as in Ref. [2] which is for aluminum, the results are comparable. In Fig. 3 the results for dimensionless deflection vs. dimensionless radius, for both simple edge and clamped edge supporting, are compared with those of Ref. [2]. As may be seen in this figure, the results are in good agreement, so the present DQM is a valid numerical scheme for the problem.

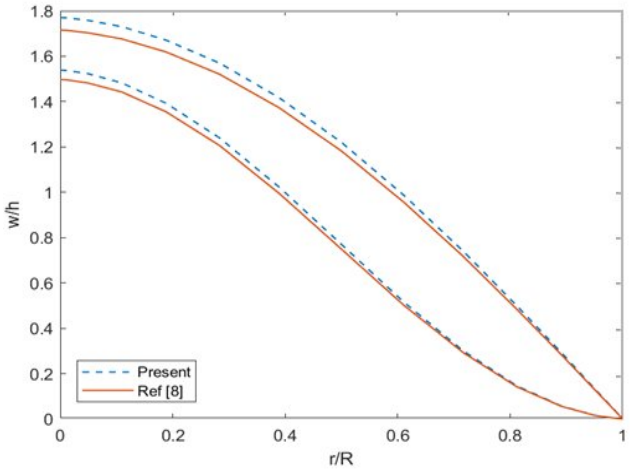

Fig. 3
Comparison of the results of present DQM, for dimensionless deflection variations vs. dimensionless radius, with those of Ref.[2] for both simply supported and clamped edge.

4.3 Parametric study

Parametric study is carried out to investigate the effects of a number of parameters on the plate deflection and buckling behavior. The parametric survey includes both clamped and simply supported boundary conditions. These surveys are shown diagrammatically in Figs.(4–8).

Fig. 4 indicates the distribution of the dimensionless deflection vs. dimensionless radius for (a) clamped and (b) simply supported edge for 5 different values of in-plane radial compressive force, *P*. As it is expected, the figure shows that the deflection increases with increase in the compressive force, Also it may be seen that the boundary conditions are satisfied. Dimensionless in-plane compressive radial Load vs. the dimensionless plate center deflection for five different values of the initial deflection is illustrated in Fig. 5. In this figure the rapid rise in the deflection at the beginning and then gradually decrease in the tangent of the curves indicates the pre-buckling zone, buckling zone as well as the post-buckling zone. Also, Fig. 5 indicates that the initial deflection has significant influence on the plate buckling and post buckling behavior. Fig. 6 shows the dimensionless deflection of plate center point vs. porosity factor for five different values of the plate elastic modulus. As can be seen in this figure, by increasing porosity and/or reducing elastic modulus, the plate deflection increases significantly. This is as one expects, since by increasing the porosity or reducing elastic modulus, the plate stiffness reduces. Fig. 7 illustrates the dimensionless deflection vs. dimensionless thickness for five different elastic moduli, (a) for clamped edge, (b) for simply supported edge. The figure indicates that by reducing the plate thickness and/or plate elastic modulus, the deflection of the plate increases in both clamped and simply supported edge conditions. Fig. 8 represents dimensionless deflection vs. dimensionless radius for five different elastic moduli for both (a) clamped edge, (b) simply supported edge condition. The figure demonstrates that by raising the dimensionless radius of the plate only a small incline in deflection takes place. However by raising elastic modulus, the plate deflection rises significantly. Fig. 9 illustrates the dimensionless deflection vs. dimensionless elastic modulus for (a) clamped edge, (b) simply supported edge condition. The figure indicates that reduction in elastic modulus causes an increase in the plate deflection. However the influence of the parameter scales down as it becomes larger and larger. Moreover the increase in simply supported plate is more significant than that of clamped plate.

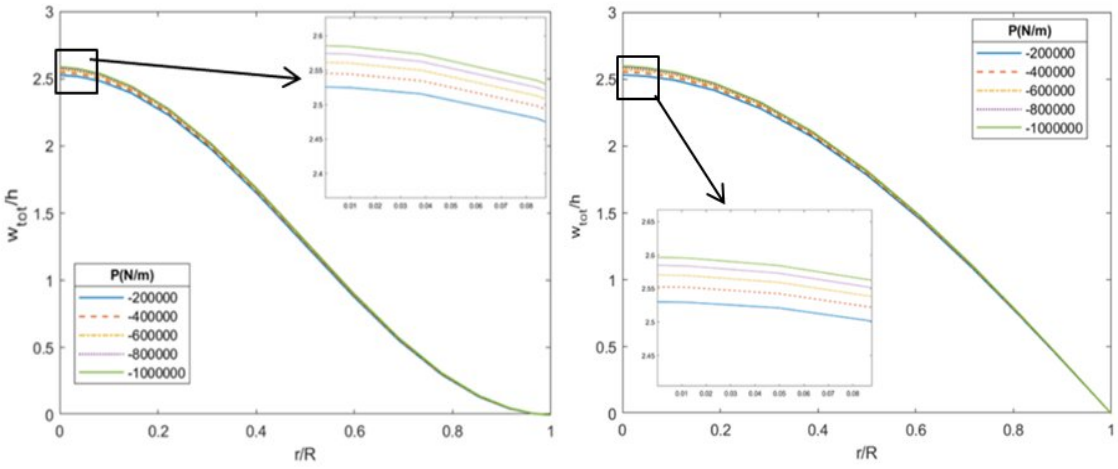

Fig. 4
Dimensionless deflection diagram vs. dimensionless radius for 5 different values of the in-plane radial compressive force (a) clamped edge, (b) simple support edge.

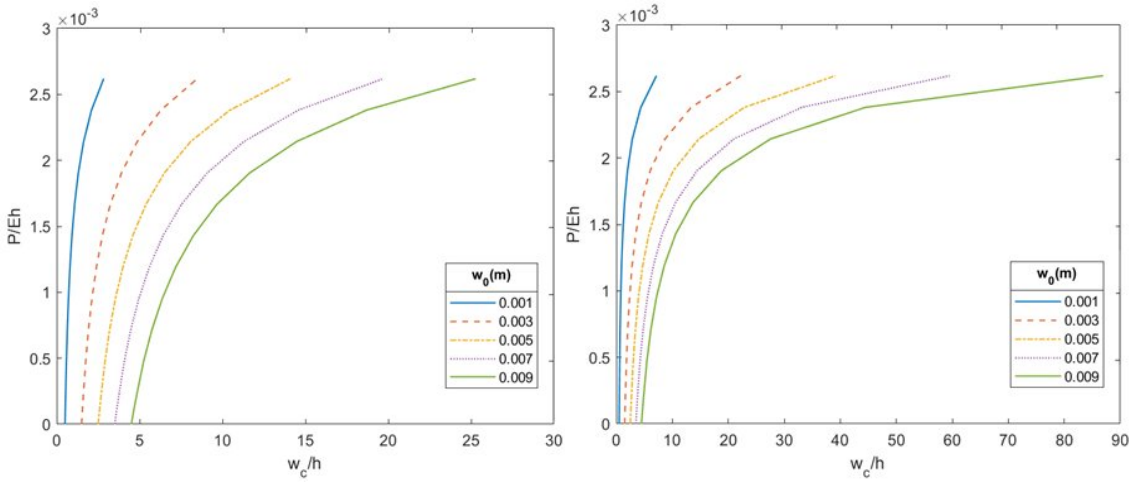

Fig. 5
Dimensionless in-plane compressive load vs. dimensionless center deflection for (a) clamped edge, (b) simply supported edge.

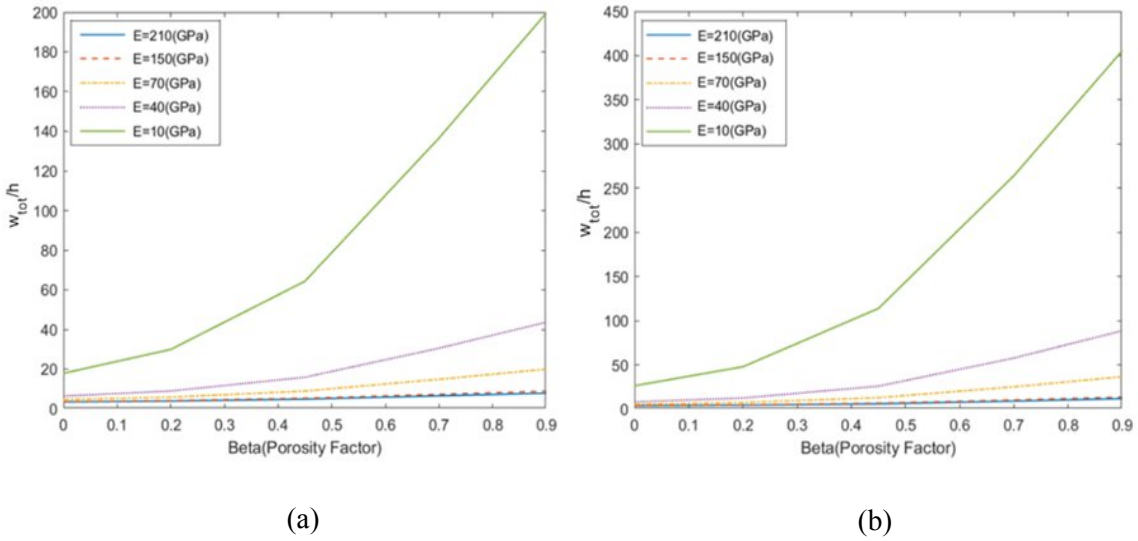

Fig. 6
Dimensionless deflection vs. porosity for 5 different young moduli for, (a) clamped edge, (b) simply supported edge.

5 CONCLUDING REMARKS

In this study, buckling and post-buckling analysis of circular porous plate with small initial deflection is investigated using the first-order shear deformation theory. Porosity is assumed non-linear in the thickness of the plate. The first-order shear deformation theory and nonlinear von-Karman strain field has been used to derive the equilibrium equations in term of displacement field. The governing differential equations together with the boundary conditions are discretized by implementing the differential quadrature method (DQM). The set of nonlinear algebraic equations are then solved for displacement field components using an iterative method. The convergence of the numerical

model is investigated. Then the comparative and parametric studies are carried out. The results show that the present DQM model has fast convergence, and accurate results. The conclusions extracted from the parametric studies are as listed in the following:

- The plate deflection increases with increase in the compressive in-plane force.
- The porosity factor has significant influence on the plate deformation.
- The illustrations indicate the pre-buckling zone, buckling zone as well as the post-buckling zone.
- The initial deflection has significant influence on the buckling, pre/post-buckling zones of the plate.
- The dimensionless deflection reduces fast by incrementing the dimensionless plate thickness.
- The dimensionless radius has small influence in the dimensionless deflection of plate.
- The dimensionless deflection decreases with increase in the dimensionless elastic modulus. However the influence of the parameter scales down as it becomes larger and larger.
- The plate boundary conditions have significant influence on the plate deflection.

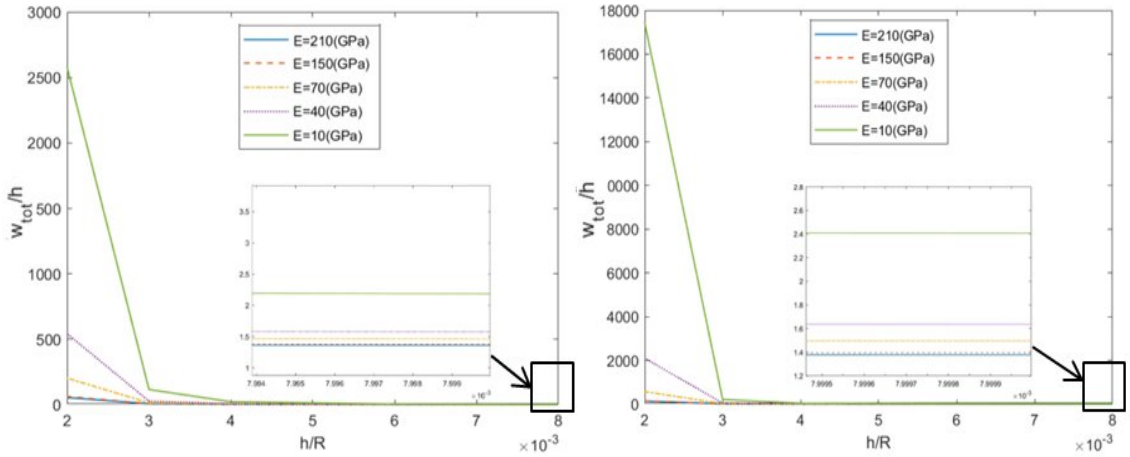

Fig. 7
Dimensionless deflection vs. dimensionless thickness for 5 different elastic moduli for (a) clamped edge, (b) simply supported edge.

ACKNOWLEDGMENT

Not applicable.

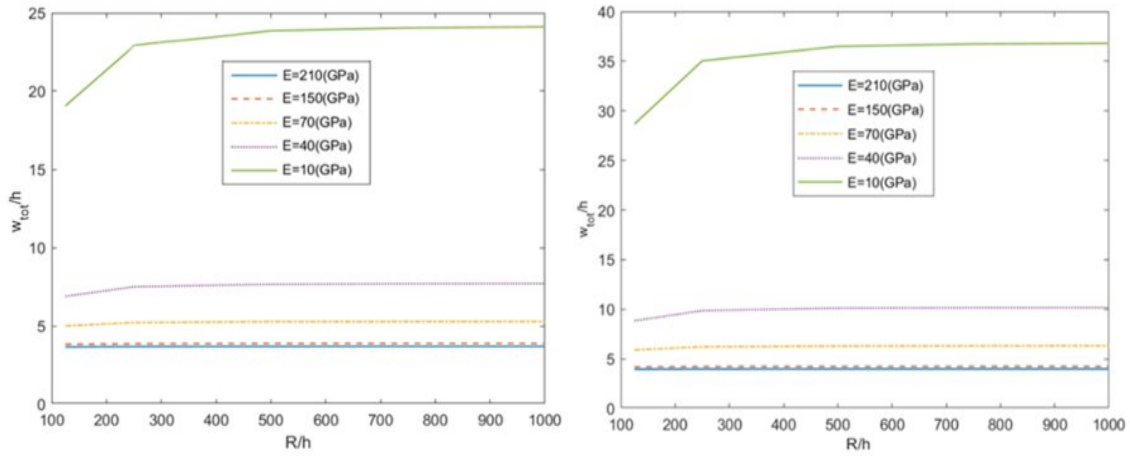

Fig. 8
Dimensionless deflection vs. dimensionless radius for 5 different young's moduli for (a) clamped edge, (b) simply supported edge.

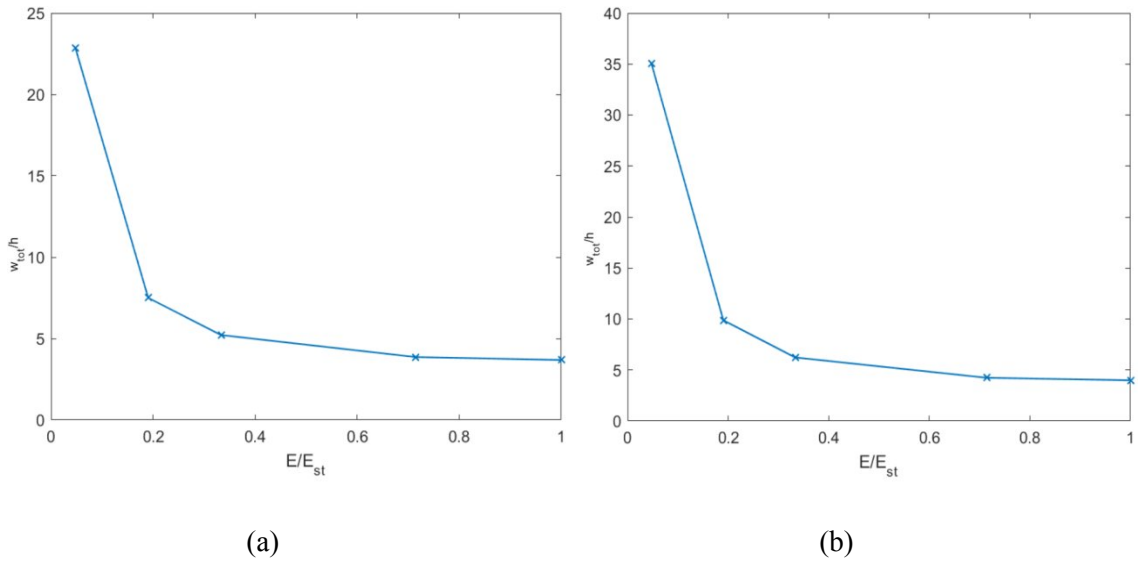

Fig. 9
Dimensionless deflection vs. dimensionless elastic modulus for (a) clamped edge, (b) simple supported edge.

REFERENCES

[1] Liu, P.S., Chen, G.F., 2014, Porous materials processing and applications.

[2] Ma, L.S., Wang, T.J., 2003, Nonlinear bending and post-buckling of a functionally graded circular plate under mechanical and thermal loadings, International Journal of Solids and Structures, Vol. 40, pp. 3311-3330

[3] Magnucki, K., Stasiewicz, P., 2004, Elastic buckling of a porous beam, Journal of Theoretical and Applied Mechanics 42, Vol. 4, pp. 859-868

[4] Samsam Shariat, B.A. and Eslami, M.R., 2005, Effect of initial imperfections on thermal buckling of functionally graded plates, Journal of Thermal Stresses, Vol. 28, pp. 1183-1198

[5] Jalali, S.K., Naei, M.H., 2010, Elastic buckling of moderately thick homogeneous circular plates of variable thickness, Journal of Solid Mechanics, Vol. 2, pp. 19-27

[6] Alipour, M.M., Shariyat, M., 2010, Stress analysis of two-directional FGM moderately thick constrained circular plates with non-uniform load and substrate stiffness distributions, Journal of Solid Mechanics, Vol. 2, pp. 316-331

[7] Magnucki, K., et al., 2010, Bending and buckling of a rectangular porous plate, Steel and Composite Structures, Vol. 6, pp. 319-328

[8] Mojahedin, A., Jabbari, M., Khorshidvand, A.R. and Eslami, M.R., 2016, Buckling analysis of functionally graded circular plates made of saturated porous materials based on higher shear deformation theory, Thin-Walled Structures, Vol. 99, pp. 83-90

[9] Kamranfard, M.R., Saeedi, A. and Naderi, A., 2018, Analytical solution of buckling of porous annular sector plates, Scientific-Research Quarterly of Aerospace Mechanics, Volume 15, Number 1, pp. 137-152 "(in Persian)"

[10] Tu, T.M., Hoa, L.K., Hung, D.X. and Hai, L.T., 2018, Nonlinear buckling and post-buckling analysis of imperfect porous plates under mechanical loads, Journal of Sandwich Structures and Materials, pp. 1-21

[11] Bagheri, H., Kiani, Y. and Eslami, M.R., 2018, Asymmetric thermal buckling of temperature dependent annular FGM plates on a partial elastic foundation, Computers and Mathematics with Applications, Vol. 75, pp. 1566- 1581

[12] Mojahedin, A., Jabbari, M. and Salavati, M., 2019, Axisymmetric buckling of saturated circular porous-cellular plate based on first-order shear deformation theory, Int. J. Hydromechatronics, Vol. 2, pp. 144-158

[13] Ghomshei, M.M., 2020, A numerical study on the thermal buckling of variable thickness Mindlin circular FGM plate in a two-parameter foundation, Mechanics Research Communications, Vol. 108

[14] Kolahi, M.R., Khorshidvand, A.R., 2021, Deflection of buckled annular porous plate, Journal of Mechanical Research and Application, Vol. 11, pp. 18-29

[15] Njim, E.K., Bakhy, S.H. and Al-Waily, M., 2021, Analytical and numerical investigation of buckling load of functionally graded materials with porous metal of sandwich plate, Materials Today: Proceedings, pp. 1-11

[16] Zenkour, A.M., Aljadani, M.H., 2022, Buckling response of functionally graded porous plates due to a Quasi-3D refined theory, Mathematics 2022, pp. 1-20

[17] Sheplak, M., Dugundji, J., To be appeared, Large deflections of clamped circular plates under initial tension and transitions to membrane behavior, Journal of Applied Mechanics

[18] Moore, D.R., Couzens, K.H. and Iremonger, M.J., 1974, The deformations behaviour of foamed thermoplastics, Journal of Cellular Plastics, pp. 135-139

[19] Jalali, S.K., Naei, M.H., 2010, Thermal stability analysis of circular functionally graded sandwich plates of variable thickness using pseudo-spectral method, Materials and Design, Vol. 31, pp. 4755-4763

[20] Saini, R., et al., 2019, Buckling and vibration of FGM circular plates in thermal environment, Proc. Struct. Integr. 14, pp. 362-374

[21] Reddy, N., 2003, Mechanics of laminated composite plates and shells theory and application 2nd edition CRC Press

[22] Ugural, A. C., 2018, Plates and shells theory and analysis fourth Edition

[23] Shu, C., Richards, B.E., 1992, Application of generalized differential quadrature to solve two-dimensional incompressible Navier-Stokes equations, International Journal for Numerical Methods in Fluids, Vol. 15, pp. 791-798